

Suppression of Band-Type Inhomogeneous Plastic Deformation in Thin Steel Plate

Research Center for Structural Materials, National Institute for Materials Science

Principal Researcher, Hai Qiu

1. Introduction

Plastic instability occurs in the deformation process of some crystalline materials in the form of single or multiple plastic bands. Piobert [1] and Lüders [2] first reported that plastic instability took place when a mild steel transitioned from an elastic to a plastic state. Portevin and Le Châtelier [3] found that plastic localization existed in a certain range of a plastic deformation process in aluminum-based alloys and low-carbon steels. Their results showed that plastic instability can take place not only in the elastic-to-plastic transition region, but also during the process of plastic deformation. The plastic instability occurring in the former period is referred to as the Lüders phenomenon, and that in the latter period as the Portevin-Le Châtelier (PLC) phenomenon. Some materials have only one of the two types of plastic instabilities [4,5], and some have both [6]. The type of plastic instability can be identified from the typical characteristic on the tensile curve: a yield plateau for the Lüders deformation [4,5] or a jerky flow (a series of serrations) for the PLC effect [7].

The Lüders deformation process is schematically shown in Fig. 1. Micro-yielding occurs at one site (Stage I), and followed by the formation of a plastic band at that site (Stage II). The band propagates across the whole area (Stage III). The formation of a plastic band was regarded to be associated with the pinning and unpinning of dislocations around the interstitial C and N.

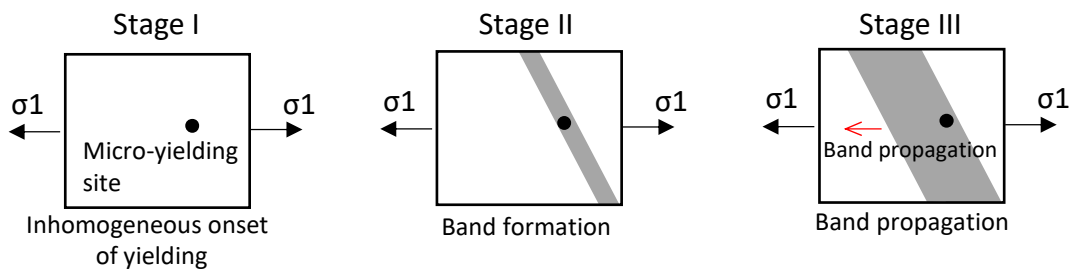


Fig. 1 Schema of inhomogeneous plastic deformation (Lüders deformation)

Based on the understanding on the micromechanism of the formation of a plastic band and the exhibition of the Lüders deformation on the stress-strain curve, two conventional measures (Method 1 and Method 2) were taken to suppress the Lüders

phenomenon (cf. Fig. 2). In method 1, IF steel in which the amount of C and N was controlled as low as possible was developed. Although decreasing the amount of C and N can lower the possibility of the formation of plastic bands, the Lüders phenomenon is still present. In method 2, by using skin-pass mill, plastic pre-strain was introduced over the whole bulk material to make the material exceed the yield plateau region. The skin-pass processed steel has a round stress-strain curve, and it completely suppressed the Lüders phenomenon. However, the large plastic pre-strain (2.23%) (almost two times the Lüders elongation) decreases the resistance to fracture.

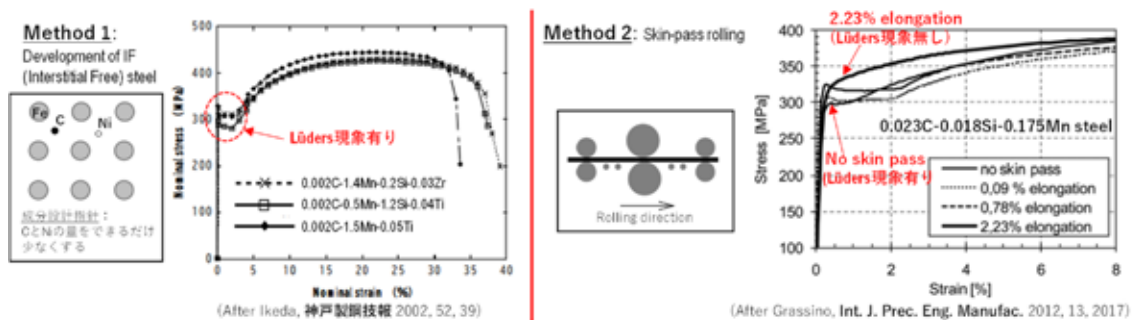


Fig. 2 Conventional methods for suppressing Lüders phenomenon

Steel has several elementary microstructures, such as ferrite, austenite, bainite, martensite, and pearlite. The Lüders phenomenon is known to occur in the ferrite [8] or austenite [9] phase, and the strain-induced phase transformation from metastable austenite to martensite leads to the PLC effect [10]. Due to the presence of ferrite or austenite, plastic instability can also take place in multi-phase steels containing either phase, e.g., ferrite/pearlite steel [4,5], ferrite/austenite steel [2,6], and ferrite/austenite/martensite steel [10]. However, the possible occurrence of plastic instability in phases other than ferrite and austenite has not been reported in the literature. The tempered martensite is a common phase for medium carbon steel. The investigation on the inhomogeneous plastic deformation in medium carbon martensitic steel is one object of the present study.

In metal forming process, occurrence of inhomogeneous plastic deformation, especially band-like plastic deformation (i.e., Lüders phenomenon), lowers the surface quality. Therefore, this kind of inhomogeneous plastic deformation is expected to be suppressed. Because the conventional measures shown in Fig. 2 have some shortcomings, a new measure is expected. In commercial steels, less local sites are suitable to form microyielding. Due to this reason, microyielding often takes place at specific local sites, and correspondingly macroscopic yielding occurs and propagates at

these local sites, resulting in inhomogeneous plastic deformation. Based on this fact, a concept is proposed in Fig. 3 that if sufficient local sites are provided for microyielding, microyielding will take place simultaneously at everywhere in the elastic region instead of a local site, and as a result, the formation of a plastic band will be suppressed, and plastic deformation proceeds homogeneously. In this study, verifying the validity of this concept in tempered martensite is another object.

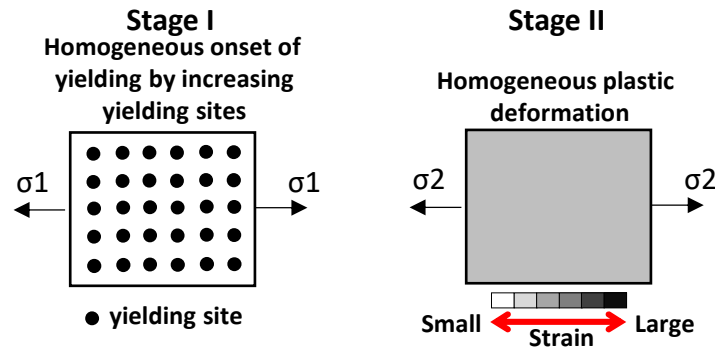


Fig. 3 Concept of suppression of inhomogeneous plastic deformation

2. Experimental

2.1 Preparation of thin steel plate

An ingot with the chemical composition of 0.3 C, 1.5 Mn, and the balance Fe (in wt%) was hot rolled to produce a thin steel plate with the cross-section of 60 mm wide and 1.6 mm thick. The hot-rolled thin steel plates 120 mm long \times 60 mm wide \times 1.6 mm thick were heat treated to prepare the following samples.

(1) The samples for evaluating the inhomogeneous plastic deformation in martensite

Tempered martensite steel plates (QT steel) were prepared by the heat treatment shown in Fig. 4. Since Lüders phenomenon in ferritic steel has been well investigated, ferritic steel was selected as a reference steel. Ferritic steel plates (F steel) were also produced (cf. Fig. 4).

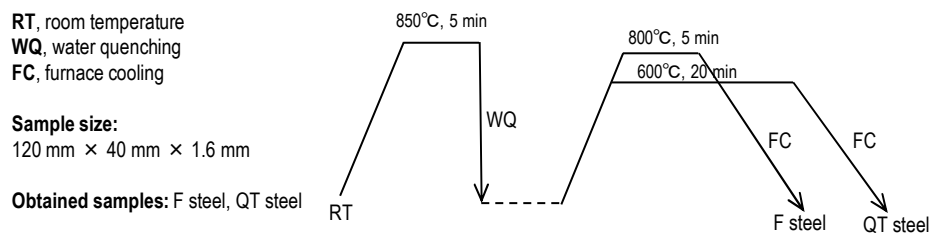


Fig. 4 The heat treatment processes and the obtained samples

(2) The samples for verifying the proposed measure of suppressing the Lüders phenomenon

Martensite phases with different dislocation densities were produced by the heat treatment processes shown in Fig. 5. Four types of samples (S1 to S4) were prepared.

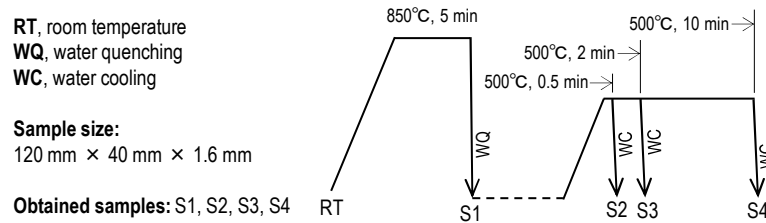


Fig. 5 The heat treatment processes and the obtained samples (S1 to S4)

The microstructures of the steel plates were examined by EBSD.

2.2 Tensile test

Dog-bone-type specimens with a parallel part 30 mm long, 8 mm wide, and 0.8~0.9 mm thick (cf. Fig. 6) were machined from QT steel (two specimens, and their numbers: QT-1 and QT-2) and F steel (two specimens, and their numbers: F-1 and F-2). Tension tests were performed at room temperature and at a crosshead speed of 0.01 mm/s.

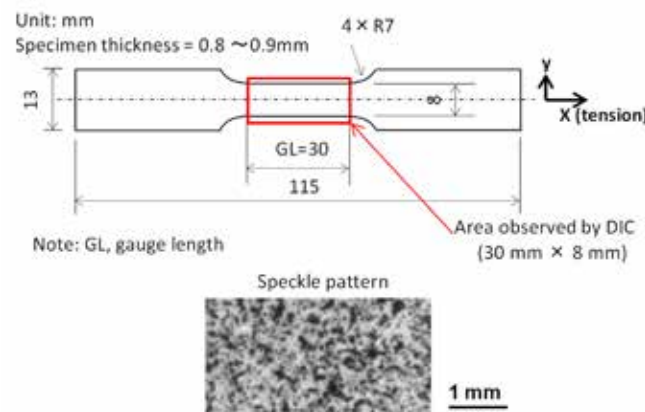


Fig. 6 The size of the dog-bone-type specimen and the spackle patterns on the front surface of the specimen

2.3 Plastic deformation measurement by digital image correlation

The front surfaces of the tensile specimens were sprayed with white and black paint to make speckles for DIC analysis. An extensometer with a gauge length (GL) of 30 mm (equal to the length of the parallel part of the specimen) was attached to the back surface.

The deformation process on the front surface was recorded successively at a time interval of 0.5 s using a camera. The digital images (area: 30 mm × 8 mm) obtained were processed using VIC-2D software with a subset size of 9 pixels × 9 pixels (246 μm × 246 μm) and a step of 5 pixels (137 μm) to produce the displacement field, strain field, and strain-rate field. In the DIC operation, the displacement uncertainty is 0.02 pixels. The DIC measurement area covers the whole GL. In the present study, the two results were obtained from tension tests: (1) macroscopic stress-strain curves showing the global image of tensile property; and (2) the evolution of plastic deformation in terms of the strain field and strain-rate field.

3. Results

3.1 Lüders deformation in tempered martensite

Two tension tests were carried out for each steel. The obtained macroscopic stress-strain curves that show the average deformation behavior over a gauge length of 30 mm are given in Fig. 7. To clearly identify the individual curves of one steel, the two curves (F-1 and F-2, QT-1 and QT-2) were intentionally placed 0.05 away from each other along the macroscopic strain axis. The microstructures of F steel and QT steel are shown in Fig. 7.

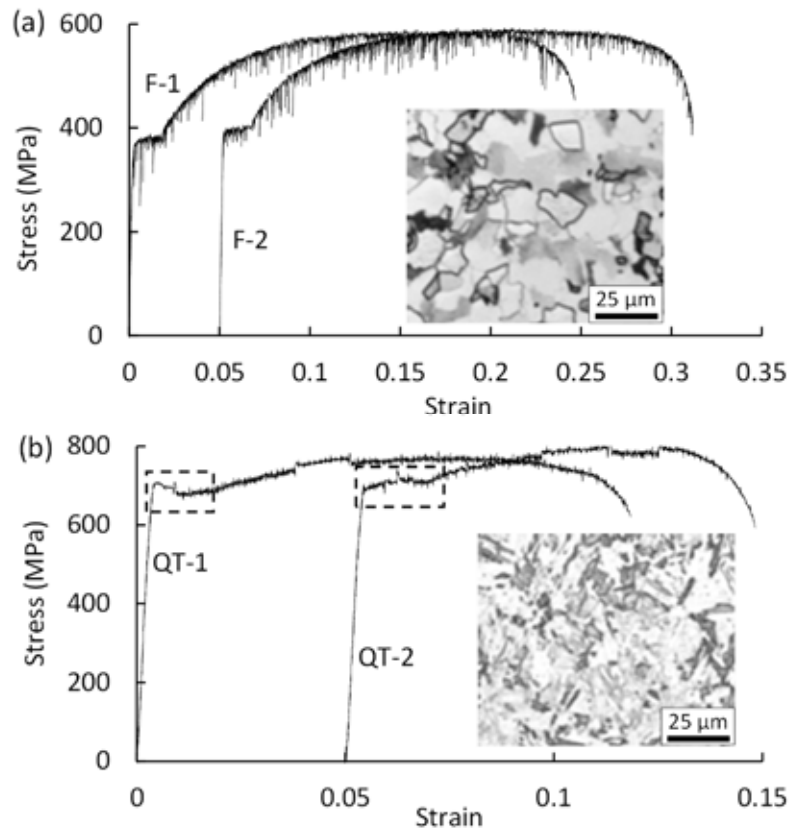


Fig. 7 Macroscopic stress-strain curves of (a) ferrite/pearlite steel (F steel) and (b) tempered martensite steel (QT steel)
 Two tests were performed for each steel (F-1 and F-2 for F steel; QT-1 and QT-2 for QT steel)

The stress-strain curve of F steel shows a typical characteristic of Lüders deformation, i.e., a yield plateau. This means that the Lüders phenomenon inevitably occurs in F steel. In contrast to F steel, the stress-strain curve of QT steel does not show clear evidence of Lüders deformation and the PLC effect. This indicates that the occurrence of plastic instability in QT steel cannot be identified only from the stress-strain curve. Digital image correlation was used to analyze the plastic deformation behavior in the following section. It is noted that a region of the stress-strain curve of QT steel is enclosed with a dotted rectangle. It was found that plastic instability takes place in the rectangle, which will be described in detail later.

Lüders deformation or the PLC effect is characterized by the plastic band. Previous studies [4,5] showed that the strain-rate field can effectively identify the moving plastic bands. In the present study, the deformation process on the front surface of tension specimens was digitalized by a camera, and the obtained digital images over the whole

tension process were used to analyze the strain and strain-rate field using two-dimensional DIC. The analysis via the strain-rate field for the F steel and QT steel shows that the plastic band occurs in two regions: (1) the elastic-to-plastic transition region (i.e., the Lüders phenomenon), and (2) the region after the onset of the necking of the tension specimen. This means that before the onset of the necking of the specimen, only the Lüders phenomenon exists in both steels. It is well known that the necking of the specimen induces plastic instability. This kind of plastic instability is not our concern, and it will not be discussed in the present study.

For the F steel, the Lüders phenomenon occurs mainly on the yield plateau. Eleven images (image ① to image ⑪) on the yield plateau of the F-1 specimen (cf. Fig. 8)

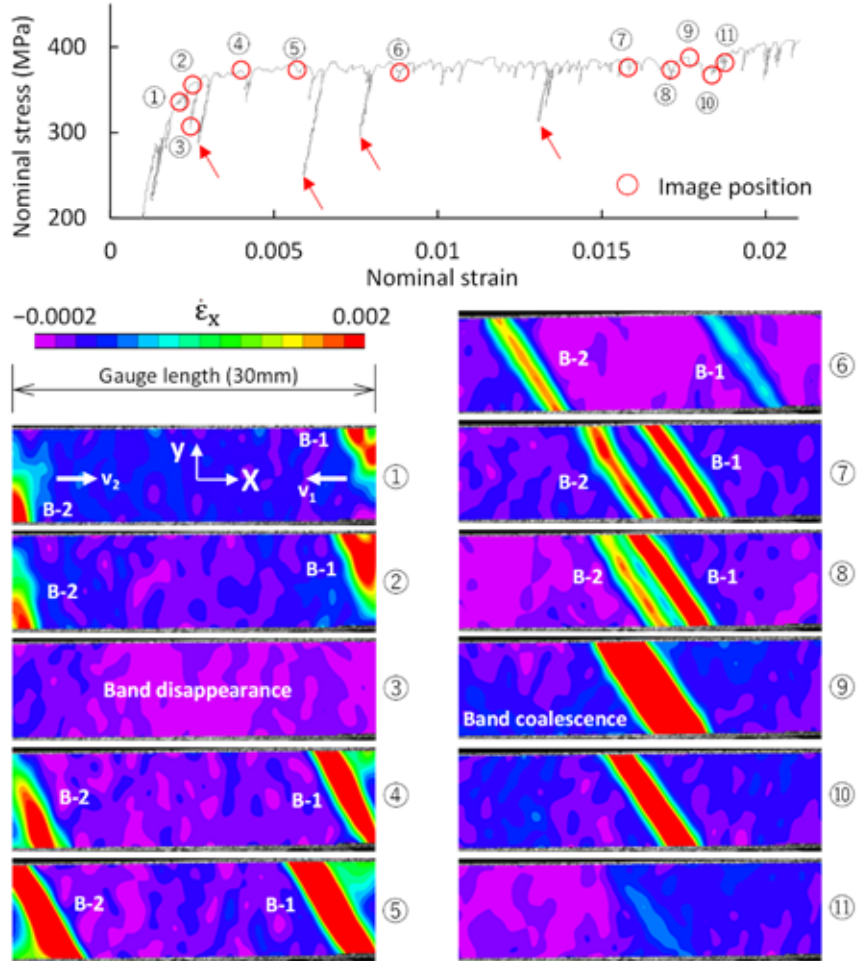


Fig. 8 Evolution of plastic bands in ferrite/pearlite steel (F-1 specimen)
 Eleven images (① to ⑪) on the macroscopic
 stress-strain curve were taken

were selected, and their strain-rate fields over a gauge length of 30 mm are shown in Fig. 8. It is generally believed that the pinning and the unpinning of dislocations cause the formation of a Lüders band. To form a Lüders band, a certain level of stress is required. Apparently, at a given applied stress level, a site with a high stress concentration more easily meets this critical stress condition than do other sites with low stress concentrations. The shoulder of a specimen produces a high stress concentration, as a result, providing an appropriate site for Lüders band nucleation. As shown in image ①, two plastic bands (B-1 and B-2) have been formed near the right and left shoulders of the specimen. It can be seen that the position of image ① on the stress-strain curve is ahead of the yield point. This indicates that plastic bands have been formed ahead of the yield point, which agrees with the observations of the previous study [4,5].

After band nucleation, B-1 propagates from right to left, while B-2 propagates toward the right. Lüders band propagation is characterized by the moving of a leading band front into the adjacent elastic region. It is also a repeated process of pinning and unpinning of dislocations. Naturally, the applied stress is required to exceed a critical stress level. Band propagation velocity has been reported to be related to the magnitude of applied stress [4]. As shown in Fig. 7, the applied stress on the yield plateau essentially remains constant, but it fluctuates significantly at some points on the yield plateau, and the applied stresses greatly decrease at those points. The applied stress corresponding to image ③ is too low to exceed the required critical stress for unlocking the dislocations, resulting in band disappearance. The strain-rate field of image ③ verifies the disappearance of the two plastic bands. When the applied stress recovers to its original value, the two bands appear again at the original sites. In Fig. 8, four arrows show four low stress levels. The two bands also disappear around the four stress levels. B-1 and B-2 propagate oppositely, until coalescing with each other (cf. image ⑨). The position of image ⑪ is nearly the end of the yield plateau, and the coalesced band almost disappears at this point.

The deformation process of QT steel over the whole stress-strain curve was examined via DIC. It was found that plastic instability occurred only within a certain range of the stress-strain curve. The range is enclosed in Fig. 7 by a dotted rectangle. The QT-1 specimen was taken to show in detail the evolution of the plastic instability in QT steel. Twenty typical points on the macroscopic stress-strain curve of the QT-1 specimen were selected (cf. Fig. 9). The strain-rate fields corresponding to the 20 points (image ① to image ⑳) are given in Fig. 9. It can be seen that two bands (B-1 and B-2) have formed near the left and right shoulders of the specimen in image ①, respectively. The position

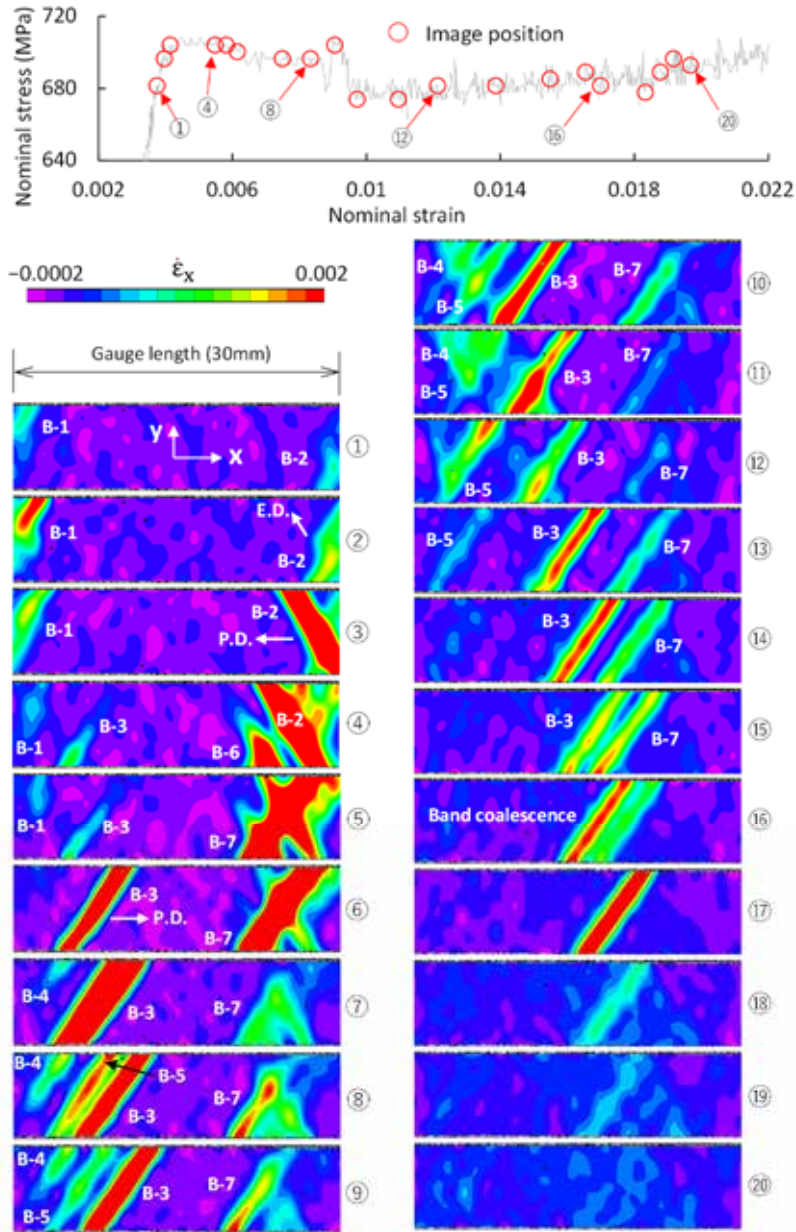


Fig. 9 Evolution of plastic bands in tempered martensite steel (QT-1 specimen) E. D., extension direction; P. D., propagation direction

of image ① in the stress-strain curve indicates that a band nucleated ahead of the yield point. The variation in the value of the strain rate within B-1 from image ① to image ⑥ shows the evolution of B-1, in that the band first grows (①→②), and then decays, and finally completely disappears (②→⑥). The position of B-1 in images ①→⑤ is almost unchanged. This indicates that the band formation, growth, and disappearance of B-1 took place at almost the same site, and apparently band propagation did not occur.

After band formation, B-2 grows along one direction from image ① to image ②, and

then extends along another direction, shown by an arrow in image ②, instead of in its original direction. Image ③ shows the appearance of B-2 after the change in the direction of extension. B-2 propagates from right to left from image ③ to image ④. In image ④, a new band (B-6) on the left side of B-2 has been formed. B-6 and B-2 coalesced and extended across the width of the specimen to produce a new band with several branches (B-7) in image ⑤. The position of B-7 is almost unchanged from image ⑤ to image ⑮. This indicates that B-7 did not propagate after band formation.

A band (B-3) was formed in image ④, which is after the upper yield point. This band extends across the width of the specimen from image ④ to image ⑥ and then propagates from left to right. In image ⑧, a new band (B-5) was split out of B-3, and B-3 continues to propagate until coalescing with B-7 in image ⑯. The coalesced band gradually decays and finally disappears. The split band (B-5) gradually decays without band propagation and finally disappears in image ⑭. B-4 experiences a process of band formation, growth, and disappearance from image ⑦ to image ⑬ that is similar to B-1 and B-5. It can be seen from Figs. 8 and 9 that the Lüders deformation process in QT steel is more complicated than that in F steel.

Because Lüders deformation occurs in the elastic-to-plastic transition region, the plastic region and the elastic region are simultaneously present in the Lüders deformation process. This indicates that the strain distribution over the specimen is heterogeneous. In Fig. 10, one point on the stress-strain curve of (a) F steel (F-1 specimen) and (b) QT steel (QT-1 specimen) that is nearly in the middle of Lüders deformation process is selected. The strain heterogeneity in the two steels is revealed by analyzing the strain distribution at this point. The experimental data of the F-1 specimen and the QT-1 specimen at this point are summarized in columns (a) and (b), respectively.

The strain-rate ($\dot{\epsilon}_x$) field of the F-1 specimen (cf. Fig. 10(a2)) shows that two moving plastic bands exist. The corresponding strain (ϵ_x) field was described in terms of two-dimensional contour (Fig. 10(a3)). The strain field is roughly divided into three regions: the middle is the elastic region, and the others are plastic regions. To quantitatively describe the strain distribution, a center line (line AB) is drawn in the two-dimensional strain contour, and the strain (ϵ_x) along the line is extracted and shown in Fig. 10(a4). Three reference points, which were directly derived from the macroscopic stress-strain curve, are also given: the Lüders strain (ϵ_L), the average strain over the gauge length (GL), and the elastic limit. The Lüders deformation process is characterized by the formation of Lüders bands (single or multiple bands), followed by band propagation over the whole specimen. The strain corresponding to the ending point of the Lüders

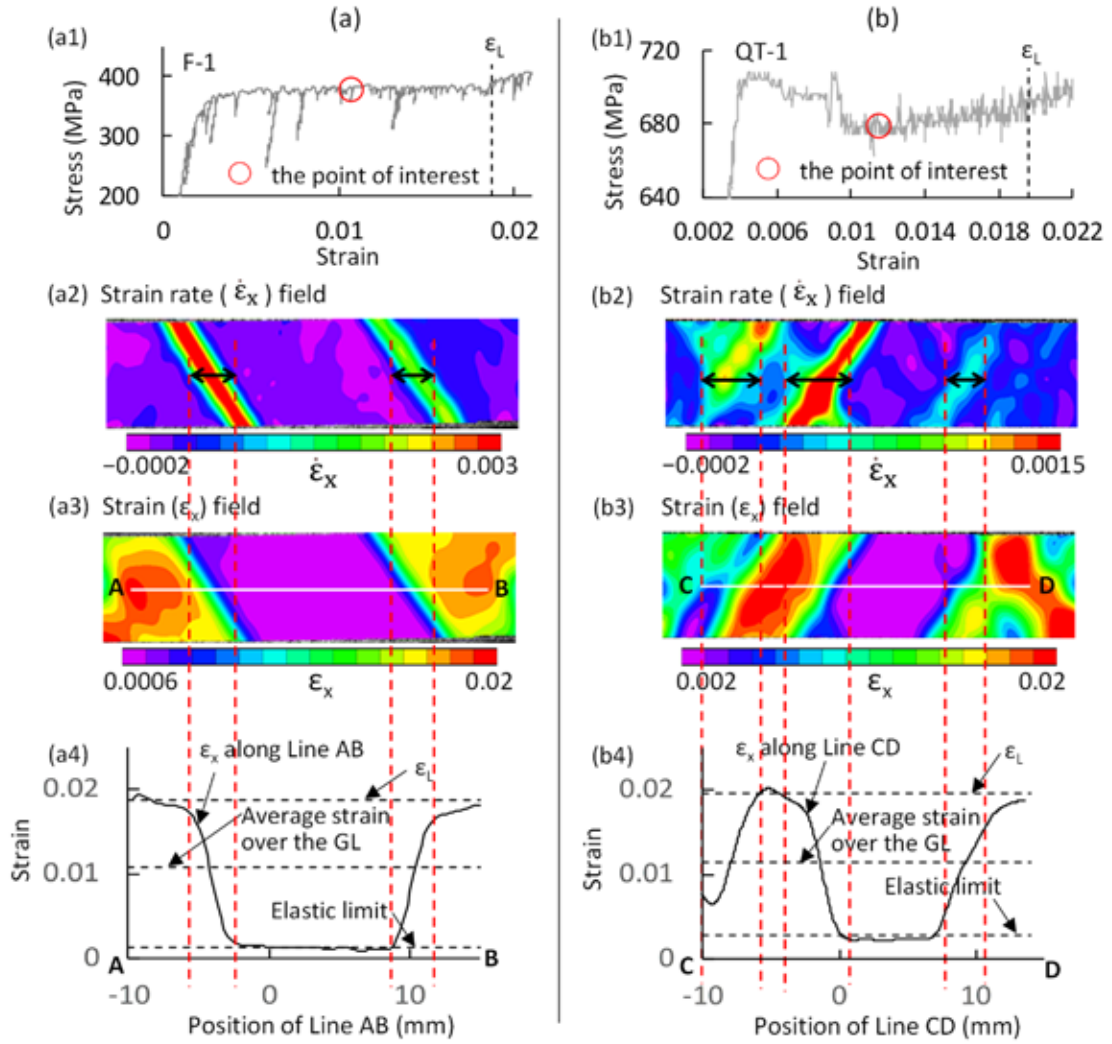


Fig. 10 Local strain (ϵ_x) distributions in (a) F steel (F-1 specimen) and (b) QT steel (QT-1 specimen) over the gauge length at a point on the macroscopic stress-strain curve located at almost the middle of the Lüders deformation process. The local strain (ϵ_x) distributions along the AB and CD lines were extracted. The average strain over the GL is the macroscopic strain of the stress-strain curve corresponding to the point of interest. ϵ_L , Lüders strain.

deformation process is referred to as the Lüders strain. For the steel with a clear yield plateau, the ending point of the Lüders deformation process is generally around the ending point of the yield plateau. This point in F-1 and QT-1 specimens was directly determined by the strain-rate field in the present study. The average strain over the GL is the macroscopic strain of the stress-strain curve of the F-1 specimen corresponding to the point of interest. Careful examination of the macroscopic stress-strain curve in the macroscopic elastic region (i.e., from point zero to the upper yield point) shows that

stress linearly increases with strain only within the initial region (from point zero to a certain stress level); beyond this region, stress gradually deviates from this straight line. The maximum macroscopic strain of the linear range is denoted as the elastic limit.

Fig. 10(a4) shows that the middle region is in the elastic state, and the corresponding strain is almost equal to the elastic limit. The width of the two moving plastic bands with respect to Line AB is marked by an arrow (\leftrightarrow) in Fig. 10(a2). The range of Line AB enclosed by the band width is shown by two vertical dotted lines in red in Figs. 10(a3) and (a4). Fig. 10(a4) shows that the strain varies significantly within the band width from an elastic strain to a large plastic strain (close to the ϵ_L). The average strain over the GL is the average value of the elastic and plastic regions.

The strain heterogeneity in the QT-1 specimen was analyzed in a similar way in Fig. 10(b). As shown in Fig. 10(b2), the shape of the moving bands is more complicated than that in the F-1 specimen. The local strain along Line CD (cf. Fig. 10(b3)) is shown in Fig. 10(b4). The strain in the elastic region (middle region) is close to the elastic limit. The width of three moving bands with respect to Line CD is shown by an arrow (\leftrightarrow) in Fig. 10(b2). The strain variation within the band width is similar to that in the F-1 specimen. The maximum plastic strain within the band width also approaches the ϵ_L . The strain distribution in the QT-1 specimen is more complicated than that in the F-1 specimen.

3.2 Suppression of Lüders deformation

Four samples (S1 to S4) were prepared. They have the same microstructure (martensite), but their dislocation density is different (the dislocation density of S1 > that of S2 > that of S3 > that of S4). The plastic deformation processes in the four samples were measured via tension test. The macroscopic stress-strain curves are shown in Fig. 11. It can be seen that for the four samples, as the dislocation density decreases, the strength gradually decreases, and the shape of the stress-strain curve changes.

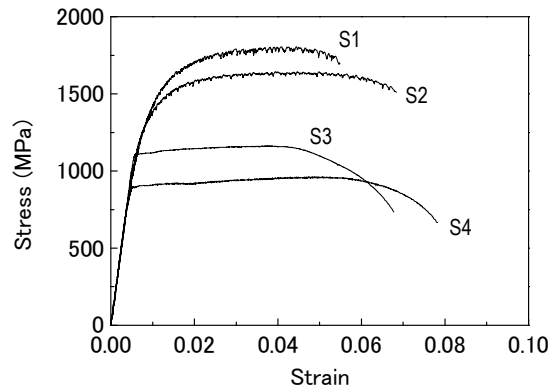


Fig. 11 Macroscopic stress-strain curves of various martensite phases

The evolution of plastic deformation over the whole front surfaces of tensile specimens was measured with the DIC technique. It was found that Lüders phenomenon was not present in S1 and S2, but was present in S3 and S4. The proof stress point ($\sigma_{0.2}$) on each stress-strain curve shown in Fig. 11 was selected. The strain rate field corresponding to this point is shown in Fig. 12. It is shown that plastic band is only present in S3 and S4. This result indicates that plastic instability can be suppressed by controlling dislocation density.

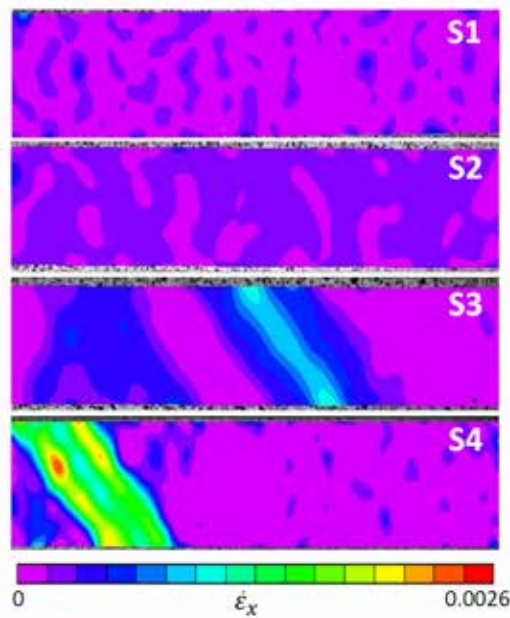


Fig. 12 The plastic strain distribution in S1 ~ S4 samples at the stress point of the proof stress ($\sigma_{0.2}$)

4. Conclusions

The plastic deformation behavior of medium-carbon tempered martensite steel at room temperature has been investigated. The results obtained regarding the plasticity of tempered martensite were as follows.

- (1) The Lüders deformation phenomenon is present, but the Portevin-Le Châtelier phenomenon is not found in the medium-carbon tempered martensite steel.
- (2) The elastic and plastic regions are simultaneously present in the Lüders deformation process. The local strain in the elastic region is close to the elastic limit. The variation in strain within a Lüders band is significant, monotonously increasing from an elastic strain to a large plastic strain that is close to the Lüders strain.
- (3) The local strain distribution in tempered martensite steel during the Lüders deformation process is more complicated than that in ferrite steel.
- (4) Lüders deformation can be suppressed by controlling the dislocation density.

Acknowledgments

This study was supported by the Technical Research Aid of JFE 21st Century Foundation. The grants are greatly appreciated.

Reference

- [1] Piobert, *Mémoire de l'Artillerie* 5(1842)502.
- [2] W. Lüders, *Dingler's Polytechnic Journal* 155(1860)18–22.
- [3] A. Portevin, F. Le Châtelier, *Comptes Rendus del Académie des Sciences de Paris* 176(1923)507.
- [4] H. Qiu, T. Inoue, R. Ueji, *Mater. Sci. Eng. A* 790(2020)139756.
- [5] H. Qiu, T. Inoue, R. Ueji, *Metals* 10(2020)530.
- [6] A. Kozłowska, B. Grzegorzcyk, M. Morawiec, A. Grajcar, *Materials* 12(2019)4175.
- [7] K. Renard, S. Ryelandt, P. J. Jacques, *Mater. Sci. Eng. A* 527(2010)2969–2977.
- [8] N. Tsuchida, H. Masuda, Y. Harada, K. Fukaura, Y. Tomota, K. Nagai, *Mater. Sci. Eng. A* 488(2008)446–452.
- [9] C. Q. Liu, Q. C. Peng, Z. L. Xue, M. M. Deng, S. J. Wang, C. W. Yang, *Metals* 8(2018)615.
- [10] B. H. Sun, N. Vanderesse, F. Fazeli, C. Scott, J. Q. Chen, P. Bocher, M. Jahazi, S. Yue, *Scripta Materialia* 133(2017)9–13.